Electrochimica Acta 53 (2008) 5670–5674

Contents lists available at ScienceDirect

Electrochimica Acta

journal homepage: www.elsevier.com/locate/electacta

Efficiency enhancement in dye-sensitized solar cells by in situ passivation of the sensitized nanoporous electrode with Li_2CO_3

Jingbo Zhang*,[1], Arie Zaban*

Department of Chemistry, Nano-energy Research Center, Bar-Ilan University, Ramat-Gan 52900, Israel

ARTICLE INFO

Article history:
Received 18 January 2008
Received in revised form 13 March 2008
Accepted 14 March 2008
Available online 21 March 2008

Keywords:
Dye-sensitized solar cell
In situ passivation
Lithium carbonate
Recombination suppression
Efficiency enhancement

ABSTRACT

This work entails a method to improve the performance of dye-sensitized nanocrystalline TiO_2 solar cells by adding surface passivating elements to the electrolyte. The presence of either CO_2, Li_2CO_3 or K_2CO_3 in electrolyte increases both the photocurrent and the photovoltage, resulting in higher overall conversion efficiency of these solar cells. The additives are used to form a passivation layer of lithium carbonate on the dye free surface of the TiO_2 nanoparticles and the conductive substrate. This layer suppresses the rate of the main recombination reaction between the photoinjected electrons and the oxidized ions in the electrolyte solution. While blocking part of the recombination, the lithium carbonate layer allows motion of the Li^+ ions towards the TiO_2 surface for charge screening. Consequently using this simple treatment, the conversion efficiency of dye-sensitized solar cell most improved by 17.2% (from 6.4% to 7.5%).

1. Introduction

The low cost dye-sensitized solar cells (DSSCs) have shown light-to-electric power conversion efficiency larger than 11% [1,2]. The high conversion efficiency in DSSCs is attributed to the high surface area of nanoporous electrodes that exhibit high light harvesting despite the monolayer coverage of dye molecules [3]. However, simultaneously, the high surface area increases one of the principal factors that limit the performance of DSSCs, the recombination of the photogenerated electron with the holes transferred to the electrolyte.

Several studies on the back reaction of injected electron were reported recently [4–12], and some methods to suppress recombination reaction have been suggested [2,4,13–21]. The recombination subtraction effort is aimed at two regions of the nanoporous electrode, the high surface area nanoporous semiconductor film and the uncovered area of the conductive substrate. In the semiconductor region, the recombination is enhanced by the high surface area while the low charge transfer resistance in the conductive substrate is an important factor for conversion efficiency of DSSCs. Regarding the substrate, two main approaches are utilized. One tries to minimize the exposed surface by the formation of a thin compact layer of the semiconductor used for the nanoporous film. In the other approach, a blocking material such as Phenol Polymer (PPO) was electrodeposited selectively in these pinholes utilizing the insolating nature of the semiconductor at the deposition potentials [4,13]. The blocking of the semiconductor is basically more complicated, due to the presence of the dye that needs to be connected directly to the semiconductor. Here also one may differentiate two approaches. The first approach relates to surface treatments prior to dye adsorption. For example, coating the nanocrystalline TiO_2 film with a thin layer of a second wide-band gap semiconductor that has a conduction band more negative than TiO_2 or with an electronic-insulating coating, such as Nb_2O_5, Al_2O_3, ZrO_2 and $CaCO_3$, forms an inherent energy barrier at the electrode-electrolyte interface. This surface barrier reduced the recombination rate and thus increased the conversion efficiency significantly [13–15,18,20]. Another approach relates to the blocking of dye free regions after the dye adsorption, for example, the adsorption of 4-*tert*-buytlpyridine on the dye free nanoparticles surface. This treatment increases the open circuit voltage (V_{oc}) of the DSSCs, while the short circuit current (J_{sc}) is usually reduced [2]. Despite the previous achievements, it is important to develop new methods for recombination suppression with the emphasis on simplicity, and a solution to both the semiconductor region and the conductive substrate.

Recent studies of lithium batteries show that the presence of CO_2 in the electrolyte solutions increases the batteries' performance. This improvement is attributed to efficient surface passivation by

* Corresponding authors.
E-mail addresses: jbzhang@iccas.ac.cn (J. Zhang), zabana@mail.biu.ac.il (A. Zaban).
[1] Present address: Institute of Chemistry, Chinese Academy of Sciences, Beijing 100190, China.

0013-4686/$ – see front matter © 2008 Elsevier Ltd. All rights reserved.
doi:10.1016/j.electacta.2008.03.027

Li_2CO_3 which is formed by a reaction between the Li and CO_2. Similar results were obtained for graphite electrodes that were cycled in CO_2 saturated electrolytes. The influence of the addition of CO_2 to the electrolyte solutions on the surface properties of various electrodes was rigorously studied. It was found that Li_2CO_3 is the major surface species that is formed. Its precipitation on the electrode suppresses surface reactions at the electrode-electrolyte interface [22–28].

We report here on the application of the lithium batteries' methodologies regarding surface passivation by carbonate salts to DSSCs. Saturation of the standard DSSC electrolyte with CO_2, and the addition of Li_2CO_3 or K_2CO_3, result in the increase of both V_{oc} and J_{sc} of the DSSCs. Spectral and electrochemical results show that the effect should be attributed to the carbonate salt that precipitates on the dye free electrode surface. The electronic-insolating nature of the carbonate salt suppresses the reaction rate of the photoinjected electrons that diffuse in the porous TiO_2 film. Consequently the overall efficiency was increased by more than 10% with this simple treatment.

2. Experimental

2.1. Materials

The chemical materials, $LiClO_4$, Li_2CO_3, K_2CO_3, I_2, 3-methyl-2-oxazolidinone (NMO) were purchased from Aldrich Chemical Co., and LiI, titanium(IV) isopropoxide ($Ti[OCH(CH_3)_2]_4$) were purchased from Merck Schuchardt. The dyes [*cis*-di(isothiocyanato)-bis(4,4′-dicarboxy-2,2′-bipyridine) ruthenium(II)] (N3) and[tris(4,4′-dicarboxy-2,2′-bipyridine) ruthenium(II) dichloride] (Ru470) were purchased from Solaronix SA Co. The remaining chemical materials were purchased from Chemical Technology, Inc. All the materials were used as received. F-doped SnO_2 conducting glass substrate (FTO, Libby Owens Ford, 16 Ω/□) were cleaned with extra pure water and dried with condensed air.

2.2. Dye-sensitized solar cells

The 23-nm-diameter TiO_2 nanocrystals were prepared using a hydrothermal method reported previously [29]. Briefly, hydrolysis of titanium(IV) isopropoxide in pH 2 acetic acid solution was followed by aging processes and hydrothermal treatment at 250 °C for 13 h. The TiO_2 paste for film preparation was obtained after evaporating excess water at 80 °C. The TiO_2 colloid paste was spread by a glass rod over a cleaned conductive glass, using adhesive tape as spacers. The thickness of the nanocrystalline TiO_2 film measured with a Surftest SV 500 profilometer of Mitutoyo Co. was about 6 μm. After sintering at 450 °C for 30 min, the electrodes were cooled to 80 °C, and dipped overnight in dry ethanol dye solution (0.5 mM N3 or Ru470). A sandwich-type configuration was employed to measure the performance of the DSSCs. The dyed electrode served as the working electrode and a platinized FTO sheet was used as counter electrode. Two narrow Teflon bands were used to form 50 μm distances between the two electrodes of the DSSCs. The standard electrolyte solution was 0.5 M LiI, 0.05 M I_2 in a 1:1 (volume ratio) mixture of dry acetonitrile and NMO. The concentrations of additions were 0.0025 M for Li_2CO_3 (saturation concentration) and 0.05 M for K_2CO_3. A Xe lamp calibrated to 1 sun in the 350–800 nm regions was used as a light source to illuminate the cells. An Eco Chemie model PGSTAYT20 potentiostat was employed to measure the performance of the DSSCs. Current–voltage curve was measured by scanning potential applied on DSSC from 0 V to negative at the scan rate of 5 mV/s.

2.3. Measurement

Infrared spectra were recorded by employing a Nicolet (impact 410) FT-IR spectrometer and the KBr disk method. To check formation of Li_2CO_3 layer on the surface of TiO_2 thin film by reducing CO_2 to CO_3^{2-}, the bare nanocrystalline TiO_2 thin film was polarized at −0.65 V in a three-electrode arrangement with Ag/AgCl as a reference electrode and Pt wire as a counter electrode for 50 min in acetonitrile of 0.1 M $LiClO_4$ bubbled with CO_2. After polarization, the TiO_2 sample was washed with acetonitrile and dried with condensed air, then removed out from conductive substrate with a doctor blade to obtain sample powder. The disk for IR measurement was made by pressing the mixture of the 5 mg sample and 195 mg dry KBr. According to the same weight ratio, the KBr disks of pure $LiClO_4$ and TiO_2 were made as IR measurement samples, respectively. Fluorescence spectra were recorded by using an AMINCO Bowman Series 2 luminescence spectrometer. Two dye Ru470 sensitized TiO_2 electrode were employed to fabricate the solar cell based on the standard electrolyte and the Li_2CO_3 saturated electrolyte, respectively. Two electrodes were subjected to fluorescence measurement immediately after solar cell measurement by washing out the entire electrolyte on the electrode. The absorption peak of R470 locates at 482 nm, so the excitation wavelength for fluorescence was set as 480 nm.

3. Results and discussion

Reduction of CO_2 to CO_3^{2-} in aprotic media is known from the lithium batteries literature. In recent studies, it was shown that in the presence of Li salts, dissolved CO_2 reacts on active and noble metals to form Li_2CO_3. The following mechanism of CO_2 reduction to Li_2CO_3 was proposed [26–28].

$$CO_2 + e^- + Li^+ \rightarrow CO_2^-Li^+ \quad (1)$$

$$CO_2Li + CO_2 \rightarrow OCOCO_2Li \quad (2)$$

$$OCOCO_2Li + e^- + Li^+ \rightarrow Li_2CO_3\downarrow + CO\uparrow \quad (3)$$

Most of the Li_2CO_3 precipitates on the electrode surface because of its low solubility in aprotic electrolytes. The resulting Li_2CO_3 layer is practically an electronic insulator with a relatively high transfer number for lithium ions. Standard DSSCs contain aprotic electrolytes and lithium ions (0.5 M LiI, 0.05 M I_2 in 1:1 acetonitrile and NMO in this study). The solubility of Li_2CO_3 in acetonitrile and NMO is low. The DSSC can be biased to the CO_2 reduction potential.

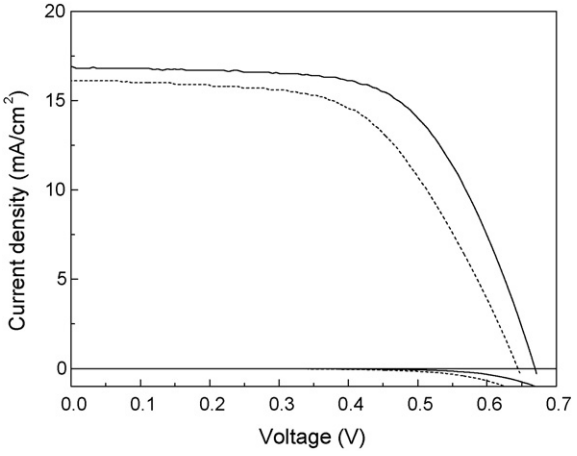

Fig. 1. Current–voltage characteristics of the DSSC which differ by the electrolyte under illumination and in the dark. The standard electrolyte: dashed line; the CO_2 electrolyte: solid line.

Therefore, it seems possible to utilize the Li_2CO_3 for the electronic isolation of both the exposed FTO surface and the dye free surface of the nanocrystalline TiO_2 electrode.

Fig. 1 shows the current–voltage characteristic of an illuminated DSSC in the presence of two electrolytes: the standard electrolyte and a standard electrolyte bubbled with dry CO_2 for 30 min (CO_2 electrolyte). The characteristic parameters for DSSC can be obtained from the current–voltage curve, such as the short circuit current (J_{sc}), the open circuit voltage (V_{oc}), the fill factor (ff, the ratio of the maximum output efficiency to the product of J_{sc} and V_{oc}) and conversion efficiency (η). The dark current–voltage curve is also provided in Fig. 1. We emphasize that both curves were measured by using the same cell simply by the replacement of the electrolyte. The use of the CO_2 electrolyte resulted in the increase of all cell parameters, i.e. J_{sc} from 16.5 to 17.2 mA/cm^2, V_{oc} from 0.664 to 0.684 V and ff from 58.1% to 63.8%. Consequently the overall conversion efficiency of this DSSC is increased by 17.2% from 6.4% to 7.5%. In addition, Fig. 1 shows that the dark current is suppressed by the use of the CO_2 electrolyte. The cell performance both under illumination and in the dark seems to indicate a decrease of the recombination rate in the cell when CO_2 is added to the electrolyte. We attribute this suppression to the formation of insoluble lithium carbonate on the non-dyed electrode surface both at the nanocrystalline TiO_2 and at the conducting substrate, as discussed below.

We attribute the Li_2CO_3 blocking of the electrode surface to its low solubility in the electrolyte. Thus, one would expect a similar effect if instead of CO_2, the electrolyte is over-saturated by Li_2CO_3. The results are shown in Fig. 2a. Here, when the standard electrolyte is replaced by a Li_2CO_3 saturated electrolyte, the V_{oc} and J_{sc} of the cell increase. The overall cell efficiency is improved by 16.9%. We also tested the effect of adding K_2CO_3 to the electrolyte. K_2CO_3 is more soluble than Li_2CO_3 and is therefore expected to behave as a less efficient surface blocker. These results are shown in Fig. 2b. Although the DSSC parameters increase by the K_2CO_3 addition, the overall conversion efficiency improvement is more moderate (10.4%) compared with CO_2 and Li_2CO_3 addition. Table 1 summarizes the performance of the three solar cells based on the standard and modified electrolytes. Table 2 presents the percentage changes of the various parameters of each cell due to the electrolyte modification. The conversion efficiency improvement order is $CO_2 > Li_2CO_3 > K_2CO_3$.

Table 1
The performance parameters of solar cells presented in Figs. 1 and 2

Electrolyte	Sample					
	1		2		3	
	Standard[a]	CO_2	Standard	Li_2CO_3	Standard	K_2CO_3
η (%)	6.4	7.5	6.5	7.6	6.7	7.4
V_{oc} (V)	0.664	0.684	0.679	0.689	0.669	0.689
J_{sc} (mA/cm^2)	16.5	17.2	16.3	18.9	16.1	17.2
ff (%)	58.1	63.8	59.0	58.7	61.7	62.3

[a] The standard electrolyte: 0.5 M LiI and 0.05 M I_2 in 1:1 acetonitrile and NMO.

Table 2
The performance enhancement percentage of the DSSCs due to different additions

	$\Delta\eta$ (%)	ΔV_{oc} (%)	ΔJ_{sc} (%)	Δff (%)
CO_2	17.2	3.0	4.2	9.8
Li_2CO_3	16.9	1.5	16.0	−0.5
K_2CO_3	10.4	3.0	6.8	1.0

As the potential is scanned negatively in the presence of both CO_2 and Li^+, CO_2 is reduced to form insoluble Li_2CO_3 which precipitates on the surface of the TiO_2 particles according to reactions (1)–(3). During voltammetry measurement, the current will decrease with formation of Li_2CO_3 due to its passivation effect. To examine this effect, a bare nanocrystalline TiO_2 electrode was employed to fabricate a sandwich-type cell with a platinized FTO sheet counter electrode, and the cell was cycled in a CO_2 containing electrolyte from 0.1 to −0.75 V *vs.* Ag/AgCl. Fig. 3 presents the current–voltage behavior of the cell during 11 consecutive cycles in the dark. The dark current decreases step by step with increasing cycle number, indicating accumulative surface passivation. We attribute the effect to the formation of Li_2CO_3 on the surface of

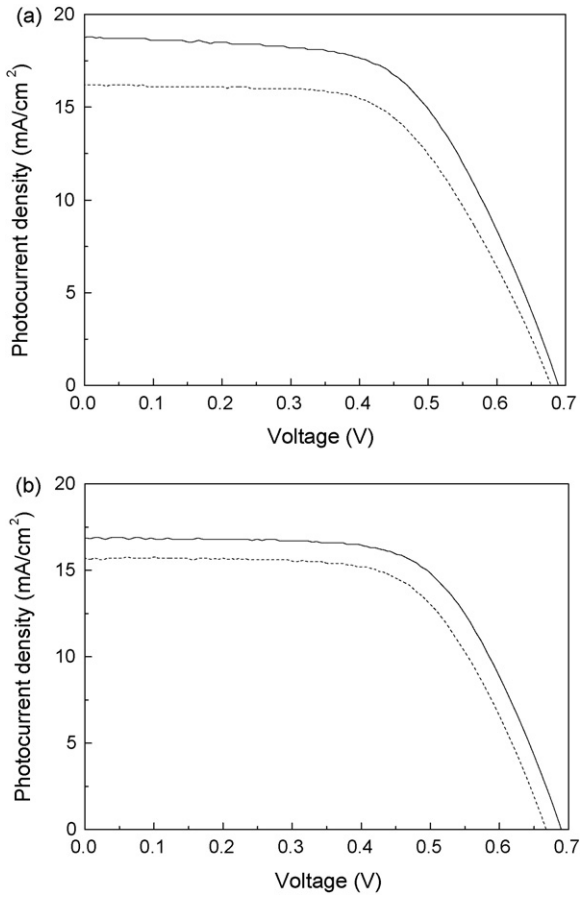

Fig. 2. Photocurrent–voltage characteristics of the DSSCs which compare the effect of the standard electrolyte with Li_2CO_3 (a) and K_2CO_3 (b). The standard electrolyte: dashed line; the electrolyte with additions: solid line.

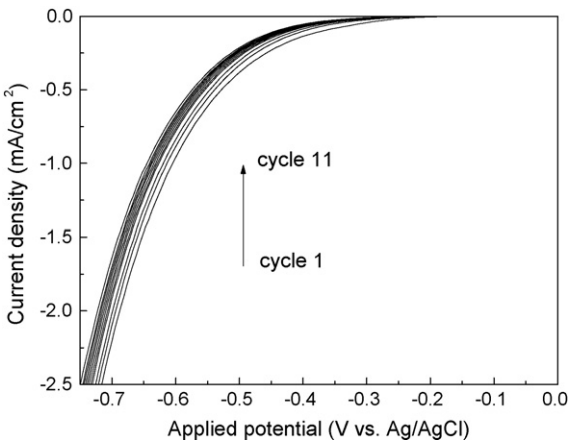

Fig. 3. A series of current–voltage curves of the nanocrystalline TiO_2 thin film cell with the CO_2 electrolyte in the dark. Scan rates: 5 mV/s.

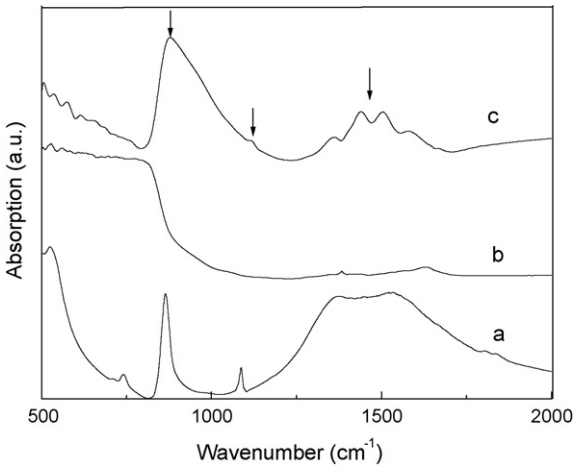

Fig. 4. FT-IR spectra of pure Li_2CO_3 (a) and TiO_2 (b) and TiO_2 coated with Li_2CO_3 (c). For pure Li_2CO_3 and TiO_2, KBr disk as background; for TiO_2 coated with Li_2CO_3, the mixture of 195 mg KBr and 5 mg TiO_2 as background. The arrow indicates the IR peak position corresponding to Li_2CO_3.

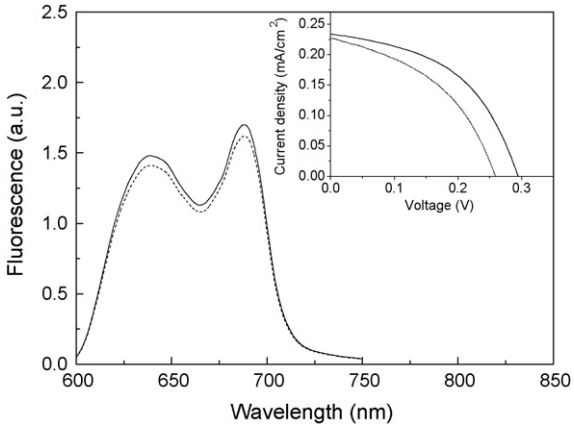

Fig. 5. Fluorescence spectra of the dye Ru470 sensitized nanocrystalline TiO_2 films after solar cell measurements in a different electrolyte. The inset: the corresponding photocurrent–voltage curves of the DSSCs. The standard electrolyte: dashed line; the Li_2CO_3 saturated electrolyte: solid line. The excitation wavelength for fluorescence was 480 nm.

the nanocrystalline TiO_2 film which suppresses the back reaction of electron with the triiodide present in electrolyte.

It is difficult to detect directly the presence of Li_2CO_3 on a dye-sensitized TiO_2 film due to the formation of trace amounts on the electrode. In order to both obtain the amount sufficient for FT-IR analysis and avoid spectral overlapping with the dye molecules, a bare TiO_2 electrode was polarized at −0.65 V *vs.* Ag/AgCl in $LiClO_4$ electrolyte saturated with CO_2. Fig. 4 (curve c) shows the FT-IR spectrum of nanocrystalline powder removed from the electrode after polarization. FT-IR spectra of pure Li_2CO_3 and TiO_2 were also recorded for comparison, and are shown in the same figure (curve a and b). Li_2CO_3 exhibits two sharp peaks at 864, 1088 cm^{-1}, and a broad peak at 1450 cm^{-1}. The nanocrystalline powder obtained from the polarized electrode exhibits peaks at 877, 1116 and 1475 cm^{-1} (marked by arrow) resembling spectra a. The small peak shift towards long wavenumber of the Li_2CO_3 present on the TiO_2 particles may be due to its adsorption on the TiO_2. These observations confirm the electrochemical formation of Li_2CO_3 on the electrode in the presence of Li^+ and CO_2.

Based on our understanding that Li_2CO_3 deposits on the TiO_2 surface between the dye molecules, we examined its effect on the electron injection process. Experiments similar to those shown above were performed using a fluorescent dye, Ru470, instead of the standard N3. Here also the performance of the DSSC was improved when a Li_2CO_3 saturated electrolyte was used (inset of Fig. 5). After we conducted solar cell measurements, we examined the fluorescence of the Ru470 sensitized electrodes. The fluorescence of adsorbed dye provides relative information regarding the injection process. A relative increase in the fluorescence indicates less efficient electron transfer from the excited state of the dye to the TiO_2. Fig. 5 shows the fluorescence spectra of the two Ru470 sensitized electrodes. The fluorescence intensity after the solar cell measurements in the Li_2CO_3 saturated electrolyte is almost similar to the intensity obtained following the cell operation in the Li_2CO_3 free electrolyte. In other words, Li_2CO_3 passivation does not interfere in the electron injection process while decreasing the rate of electron recombination.

Fig. 6 compares the V_{oc} decay of a standard DSSC with that of a cell containing Li_2CO_3 saturated electrolyte. V_{oc} decay measurements represent the recombination processes in the DSSC in a simple way [30,31]. In practice, we plot the time dependence of V_{oc} in the dark, starting with an illuminated cell. Slower decay of the V_{oc} represents a lower rate of the electrons loss processes allowing a comparison between two cells. In Fig. 6, the V_{oc} of the standard DSSC was normalized to that of DSSC containing the Li_2CO_3 saturated electrolyte to clarify the comparison. Fig. 6 shows that the recombination process is significantly slower in the DSSC containing the Li_2CO_3 saturated electrolyte. We attribute the recombination suppression to the blocking effect of the surface adsorbed Li_2CO_3. This treatment significantly improves all DSSC parameters resulting in higher conversion efficiency.

According to the above analyses, precipitation of Li_2CO_3 on the surface of the nanoporous TiO_2 can be achieved by bubbling CO_2 into a standard electrolyte followed by an electrochemical process, or by the addition of carbonate salts such as Li_2CO_3 and K_2CO_3 into the standard electrolyte. Li_2CO_3 precipitates stably on the electrode surface due to its low solubility in the DSSC electrolyte. Surface passivation in DSSC using Li_2CO_3 involves unique conditions in which electron transport across the blocking layer is blocked while the migration of small ions like Li^+ is quite good [25,27]. The latter enables the screening of the photoinjected electrons from the electrolyte solution which is a critical process in DSSCs [32]. Due to the passivation of Li_2CO_3, electron concentration in the TiO_2 increases, thus improving both the photovoltage and photocurrent of the DSSC.

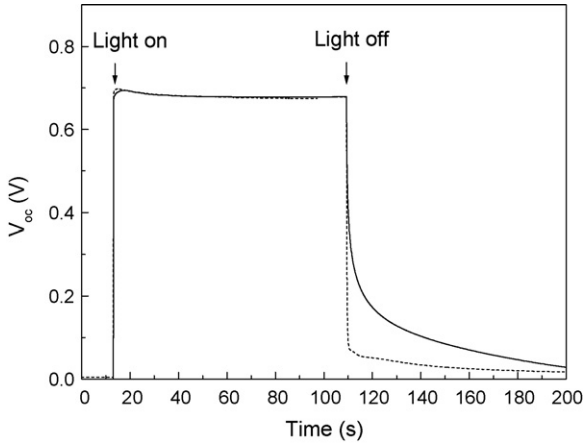

Fig. 6. V_{oc} decay curves with time for the DSSCs based on a different electrolyte. The V_{oc} of the standard DSSC (dotted line) was normalized to that of the DSSC based on the Li_2CO_3 saturated electrolyte (solid line).

4. Conclusion

The performance of DSSCs can be improved by the addition of CO_2, Li_2CO_3, or K_2CO_3 to the electrolyte. The conversion efficiency was increased by more than 10% by this simple treatment in the following improvement order: $CO_2 > Li_2CO_3 > K_2CO_3$. FT-IR results show that these additives form Li_2CO_3 on the surface of the TiO_2 nanoparticles, thus suppressing the rate of electron recombination. The formation of Li_2CO_3 on the nanoparticle surface has no effect on the electron injection process. Consequently both the photocurrent and the photovoltage of the DSSC were improved by this simple treatment.

Acknowledgements

The authors thank the Israeli Ministry of Science for the support of this work. Jingbo Zhang thanks the Kort Fund for the financial support of his project.

References

[1] B. O'Regan, M. Grätzel, Nature 353 (1991) 737.
[2] M.K. Nazeeruddin, A. Kay, I. Rodicio, R. Humphry-Baker, E. Muller, P. Liska, N. Vlachopoulos, M. Grätzel, J. Am. Chem. Soc. 115 (1993) 6382.
[3] M. Grätzel, J. Sol-Gel Sci. Technol. 22 (2001) 7.
[4] B.A. Gregg, F. Pichot, S. Ferrerre, C.L. Fields, J. Phys. Chem. B 105 (2001) 1422.
[5] N.W. Duffy, L.M. Peter, R.M.G. Rajaapakse, K.G.U. Wijayaantha, J. Phys. Chem. B 104 (2000) 8916.
[6] A.C. Fisher, L.M. Peter, E.A. Ponomaarev, A.B. Waller, K.G.U. Wijayantha, J. Phys. Chem. B 104 (2000) 949.
[7] Y. Tachibana, S.A. Haque, I.P. Mercer, J.R. Durrant, D.R. Klug, J. Phys. Chem. B 105 (2001) 7424.
[8] H.N. Ghosh, J. Phys. Chem. B 103 (1999) 10382.
[9] G. Benko, M. Hilgendorff, A.P. Yartsev, V. Sundstrom, J. Phys. Chem. B 105 (2001) 967.
[10] P. Wang, L.D. Wang, B.B. Ma, B. Li, Y. Qiu, J. Phys. Chem. B 110 (2006) 14406.
[11] J.C. Guo, C.X. She, T.Q. Lian, J. Phys. Chem. C 111 (2007) 8979.
[12] K. Takeshita, Y. Sasaki, M. Kobashi, Y. Tanaka, S. Maeda, A. Yamakata, T. Ishibashi, H. Onishi, J. Phys. Chem. B 108 (2004) 2963.
[13] S.G. Chen, S. Chappel, Y. Diamant, A. Zaban, Chem. Mater. 13 (2001) 4629.
[14] A. Zaban, S.G. Chen, S. Chappel, B.A. Gregg, Chem. Commun. (2000) 2231.
[15] K. Tennakone, G.R.R.A. Kumara, I.R.M. Kottegoda, V.P.S. Perera, Chem. Commun. (1999) 15.
[16] D.B. Menzies, Q. Dai, L. Bourgeois, R.A. Caruso, Y.B. Cheng, G.P. Simon, L. Spiccia, Nanotechnology 18 (2007) 125608.
[17] J. Xia, N. Masaki, K. Jiang, S. Yanagida, J. Phys. Chem. B 110 (2006) 25222.
[18] Z.S. Wang, M. Yanagida, K. Sayama, H. Sugihara, Chem. Mater. 18 (2006)2912.
[19] H. Alarcon, G. Boschloo, P. Mendoza, J.L. Solis, A. Hagfeldt, J. Phys. Chem. B 109 (2005) 18483.
[20] E. Palomares, J.N. Clifford, S.A. Haque, T. Lutz, J.R. Durrant, J. Am. Chem. Soc. 125 (2003) 475.
[21] D. Aurbach, A. Zaban, J. Electrochem. Soc. 141 (1994) 1808.
[22] Y. Gofer, Y.E. Ely, D. Aurbach, Electrochim. Acta 37 (1992) 1897.
[23] Y.E. Ely, D. Aurbach, Langmuir 8 (1992) 1845.
[24] D. Aurbach, A. Zaban, J. Electroanal. Chem. 393 (1995) 43.
[25] Y.E. Eineli, D. Aurbach, J. Power Sources 54 (1995) 281.
[26] D. Aurbach, Y.E. Eineli, O. Chusid, Y. Carmeli, M. Babai, H. Yamin, J. Electrochem. Soc. 141 (1994) 603.
[27] D. Aurbach, O. Chusid, J. Electrochem. Soc. 140 (1993) L155.
[28] D. Aurbach, Y. Gofer, M. Benzion, P. Aped, J. Electroanal. Chem. 339 (1992) 451.
[29] A. Zaban, S.T. Aruna, S. Tirosh, B.A. Gregg, Y. Matai, J. Phys. Chem. B 104 (2000) 4130.
[30] A. Zaban, M. Greenshtein, J. Bisquert, ChemPhysChem 4 (2003) 859.
[31] S. Chappel, L. Grinis, A. Ofir, A. Zaban, J. Phys. Chem. B 109 (2005) 1643.
[32] Y. Harima, K. Kawabuchi, S. Kajihara, A. Ishii, Y. Ooyama, K. Takeda, Appl. Phys. Lett. 90 (2007) 103517.